PHYSICS AND CHEMISTRY OF SOLID STATE
V. 23, No. 4 (2022) pp. 678-685
Section: Chemistry

DOI: 10.15330/pcss.23.4.678-685

Vasyl Stefanyk Precarpathian National University

ФІЗИКА І ХІМІЯ ТВЕРДОГО ТІЛА
Т. 23, № 4 (2022) С. 678-685
Хімічні науки

UDC: 66.017:544.-3:544.77 ISSN 1729-4428

V.G. Pylypko[1], O.V.Krupko[2] and P.M. Fochuk[1]

Influence of various capping agents on optical properties and stability of MnS nanoparticles

[1]*Yuriy Fed'kovych Chernivtsi National University, Chernivtsi, Ukraine, 58012; v.pylypko@chnu.edu.ua*
[2]*Bukovinian State Medical University, Chernivtsi, Ukraine, 58002; krupkoo@ukr.net*

Two thiols (L-cysteine and thioglycolic acid) as well as citrate-anion were employed as coordinating reagents to control the MnS nanoparticles nucleation and growth at various pH in aqueous media. The obtained colloids were characterized by means of UV–visible spectroscopy and atomic force microscopy. Mass fraction of elements was estimated by Energy Dispersive X– ray. Effect of the nanoparticles forming ions (Mn^{2+} and S^{2-}) molar ratio as well as the capping agents nature and content (the ligands coordination number *c. n.* = 2; 4 and 6) on UV–vis absorbance spectra was studied. It was determined that Mn^{2+}– ions amount and the coordination number of the stabilizers needed for effective capping of the MnS nanoparticles are close in the three studied cases. Possibility of $Mn(OH)_2$ formation as an additional product of S^{2-}- and Mn^{2+}– ions interaction in aqueous medium is discussed.

Key words: manganese (II) sulphide, nanoparticles, synthesis, L–cysteine, thioglicolic acid, citrate-ions, absorbance spectra, Atomic Force Microscopy, Energy Dispersive X–ray analysis.

Received 23 August 2022; Accepted 10 October 2022.

Introduction

Similary to bulk wide band-gap (3,1eV) magnetic semiconductor nanosized manganese sulphide MnS had attracted extensive interest for the potential applications in the field of short wavelength optoelectronics, as photoluminescent component, photocatalist, contrast agent for magnetic resonance imaging, as an alternative for anode material in LIBs [1, 2] or in medicine [3].

MnS nanoparticles (NPs) usually are synthesized by different routes including chemical vapor deposition, microwave irradiation, spray pyrolysis and, mostly, solvothermal and hydrothermal [4-10] methods. Nanosized MnS are obtained in three polymorphic forms: cubic α-MnS (stable, green), cubic β-MnS (meta-stable, pink), and hexagonal γ-MnS (meta-stable, pink) [5].

High-temperature solvothermal reaction seems to be effective for fabricating various structures of the MnS NPs, in particular, nanorods, mono- and branched wires, hollow spheres and cubes, porous networks, coral shaped and floral-like [5-9] nanostructures. However less data are available about a chemical bath deposition in aqua media at ambient temperatures [11, 12].

Short a list of substances is known as capping agents for MnS NPs, namely, L-cysteine [2, 10 and 13], citrate-ions [11], EDTA [14], palmitoyl piperidinium chloride and stearoyl piperidinium chloride [15] and starch even [12]. Multipod γ-MnS microcrystals have been synthesized by the solvothermal method with thiosemicarbazide both as sulphur source and stabilizer [8]. According to [16], α - and γ-MnS NPs formed as pure phases upon mixing of $MnCl_2$ and Na_2S aqua solutions at high temperature without the use of any organic reagents even. Thus a colloidal synthesis technique seems a simple yet effective way of MnS nanoparticles synthesizing.

The aim of this paper is to study perculiarities of MnS NPs capped by various stabilizers formation in aqua at ambient temperature. To compare a stabilizing effect on the MnS NPs of two thiols, namely, L-cysteine (L-cys) and thioglycolic acid (TGA) with action of citrate-ions the syntheses were provided at the same thermodynamic conditions.

We chose the biologically relevant agents L-cys and TGA as stabilizers for several reasons. They are soluble in

water; both contain a SH-group that in L-cys case is known as a strong binder for MnS [2], CdS and CdSe NPs' [17] surfaces; both show complex formation effect for Mn^{2+}-ions. Mercaptoacetic acid TGA is commonly used as a surface-passivating ligand in chalcogenide NPs syntheses because it enables directed nanoparticles assembly. Besides, the both ligands are carboxylic acids differing by an NH_2- amino group presence in L-cys. Contrary, potentially capping agents citrate-ions can bond to MnS NPs surface by a carboxylic group only.

I. Experimental

Manganese chloride tetrahydrate $MnCl_2{\cdot}4H_2O$ (≥99%), L-cysteine $HO_2CCH(NH_2)CH_2SH$ (≥98.5%), thioglycolic acid (TGA) $HS\text{-}CH_2COOH$ (≥99%), Trisodium citrate dihydrate $C_6H_5Na_3O_7{\cdot}2H_2O$ (later citrate) (≥99%), Sodium sulfide $Na_2S{\cdot}9H_2O$ and NaOH (≥99%) (all was purchased from Sigma Aldrich) were used unaltered for the synthesis.

Two stock aqua solutions of 0.005M (Series A) and 0.05 M (Series B) $MnCl_2{\cdot}4H_2O$ were used as precursors for the Mn/ligand complexation. While the Series A solutions were characterized by $[Mn^{2+}]:[S^{2-}]$ = 1:1 and 1:2 with the ligands coordination number *c. n.* = 2; 4 and 6, the solutions of Series B contained double excess of the anion to achieve *c. n.* = 2 only. In each Series of experiments, colloidal MnS NPs solutions were synthesized and their characteristics were investigated simultaneously.

The molar ratio of the cation, anion and the stabilizer content in the Series A experiments are collected in Table 1 on example of L–cysteine (the same ratio is in TGA and citrate-ions cases).

Table 1

Initial concentration of the precursors and their molar ratio in the mixed solutions (Series A).

N	$[Mn^{2+}]$, M	[L-cys], M	$[S^{2-}]$, M	$[Mn^{2+}]$: [L-cys]: $[S^{2-}]$
1	0,005	0,01	0,005	1:2:1
2	0,005	0,01	0,01	1:2:2
3	0,005	0,02	0,005	1:4:1
4	0,005	0,02	0,01	1:4:2
5	0,005	0,03	0,005	1:6:1
6	0,005	0,03	0,01	1:6:2

The Mn/L-cys (TGA, citrate) complexes solutions were prepared previously by the precursors stirring in an ultrasonic bath during 0.5 h at 328 K. Proper volume of the fresh prepared 0.005 M or 0.05 M Na_2S aqueous solution was added to the complexes solutions aliquot as a source of the sulfide-ions. Since the final volume of the mixtures was standardized by deionized water to 100 ml, the final $[Mn^{2+}]$ was equal to $1.25{\cdot}10^{-3}$ and $1.25{\cdot}10^{-2}$ M in Series A and B, correspondingly. Then the final solution was stirred vigorously in an ultrasonic bath at 328 K and aged for 0.5 h. First aliquots for an UV–visible analysis were taken after 0.5h mixing all precursors.

UV-vis absorbance spectra of the obtained solutions monitoring were performed at room temperature using Cary 60 Spectrophotometer (190 - 1100 nm).

The pH conditions were verified for each measurement via a digital pH meter pH-150МИ which was calibrated using standard buffer solutions.

Mass fraction of elements was determined by Energy Dispersive X-ray (EDX) fluorescence analyzer EXPERT 3L with an absolute error 0.05 - 0.2%. The obtained in Series B precipitates were filtered, diligently washed and dried by absolute ethanol from water followed by heating at 353 K. Each system was three to five times, the results were averaged.

Nanoparticles size and shape were investigated by Atomic Force Microscopy (AFM) NT-206. The obtained aqueous suspensions (0.03 ml) were put on a cleaned mica substrate and dried under the cover on the warm heating plate (≈ 313 K).

II. Results and discussion

2.1. MnS/L-cys NPs synthesis

2.1.1. Series A.

Mixing of all componets for the solutions NN1 - 6 had resulted at first in emerald hue occurrence that disapeared rapidly. After the ultrasound treatment during 0.5h all solutions remained transparent and colorless as long as a week with the exception of the solution N2 where slight pink turbid occurred after a day. Within 13 days observations of the solution N2 a brown film on the surface over the pink precipitate had appeared.

Low *c.n.* = 2 for the ligands was choosed previously based on data [18] where a stability constant ($K_{f,n}$) of $[Mn(L\text{-}cys)_n]^{2+}$ complex had been proposed as log $K_{f,1}$ and was ranged 2÷4.9 for *n* = 1 and log $K_{f,2}$= 8.62 for *n* = 2. Similar values of log $K_{f,1}$ = 4.57 and log $K_{f,2}$ = 8.23 (at 298 K) are given in [19]. However, it was interesting to study effect of the capping agent content on the MnS/L-cys NPs formation and stability therefore *c. n.* = 4 and 6 was used also.

Fig. 1a demonstrates complexity of the MnS/L-cys NPs UV-vis absorbance spectra by strong overlap between two spectra with maxima at about 205 and 235 nm for the molar ratio $[Mn^{2+}]:[S^{2-}]$ = 1:1 (or 205 and 250 nm when $[Mn^{2+}]:[S^{2-}]$ = 1:2), *c. n.* = 2; 4 and 6. One can see that the UV-vis spectra of the solutions with stoichiometric ratio $[Mn^{2+}]:[S^{2-}]$ = 1:1 at *c.n.*= 2; 4 and 6 are almost identical. The spectra of the solutions with the double S^{2-} excess ($[Mn^{2+}]:[S^{2-}]$= 1:2) at *c. n.* = 2; 4 and 6 are almost identical also however their edge moved to longer vawes as the larger NPs formation evidence. Obviously at the double $[S^{2-}]$ excess the NPs growth rate is higher at all investigated *c.n.* Similar tendency was noted in [1] were double $[S^{2-}]$ excess had positive action on MnS NPs formation by the solvothermal method. This means that twice increase of the anion content plays dominate role in the NPs growth rate while 3-fold increase of the L-cys content not influenced the NPs sizes. Variation of the complexes stock solutions pH from 7 up to 11 in experiments at *c. n.* = 2 (Fig.1b) weakly influenced the absorption edge position.

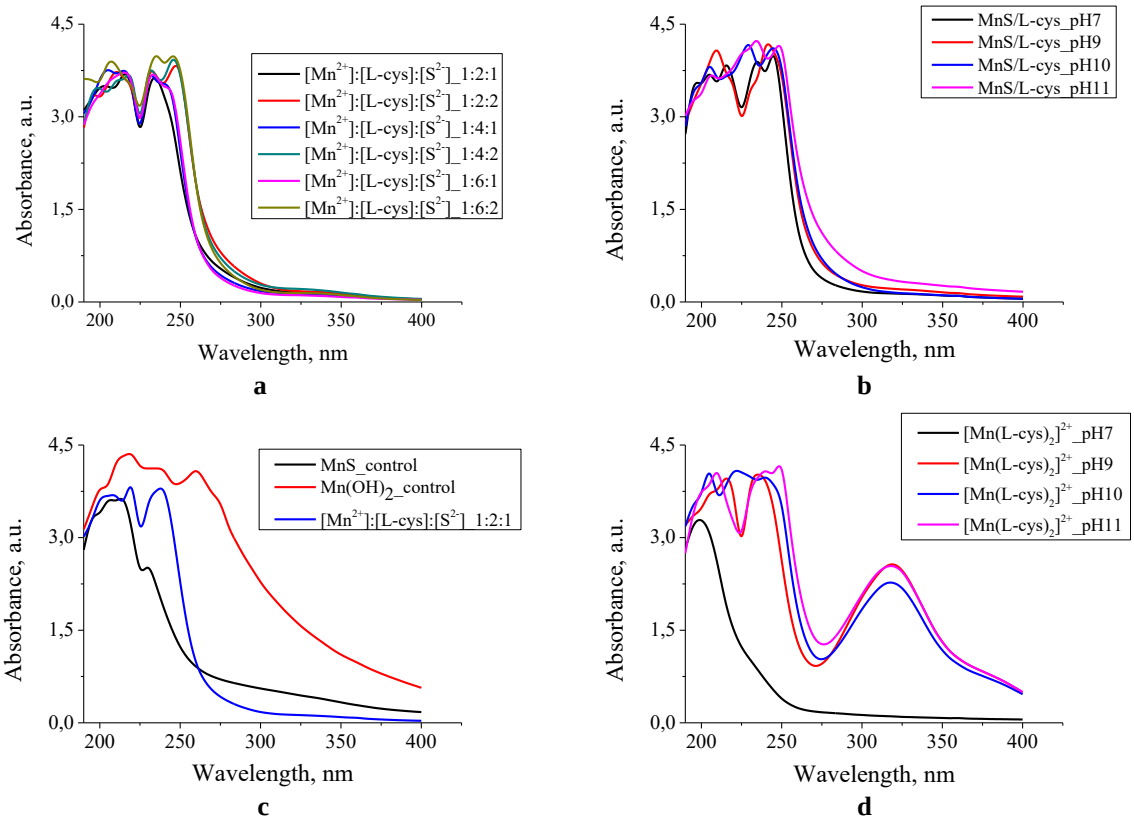

Fig. 1. a – comparison of the MnS/L-cys NPs UV–vis absorbance spectra at $[Mn^{2+}]:[S^{2-}]$ =1:1 and 1:2 and *c.n.* = 2; 4 and 6 (see legend); b – the absorbance spectra of the MnS/L-cys colloids prepared at *c. n.*=2 at pH from 7 up to 11; c – the absorbance spectra of the MnS/L-cys colloids in comparison with the spectra of the fresh control $Mn(OH)_2$ and MnS; d – the absorbance spectra of the $[Mn(L\text{-}cys)_2]^{2+}$ complex at various pH values.

Occurrence of the brown film on the solution N2 surface can be connected with oxidation of $Mn(OH)_2$ that can formed as an additional product in the basic media. Really, the Na_2S aqua stock solutions are alkaline due to the sulfide-ions hydrolysis

$$Na_2S + H_2O \rightarrow HS^- + OH^- + 2Na^+ \quad (1)$$

$$HS^- + H_2O \rightarrow H_2S + OH^- \quad (2)$$

$$Mn^{2+} + 2OH^- \rightarrow Mn(OH)_2 \quad (3)$$

This dyhydroxide is poorly soluble in water (K_{sp} = $1.9 \cdot 10^{-13}$ [20] that is less even or comparable with value K_{sp} = $3 \cdot 10^{-10}$ and $3 \cdot 10^{-13}$ for metastable and stable MnS forms, respectively [7]). Unfortunately, there is no alone opinion in literature about $Mn(OH)_2$ color (pink, grey or white according to various papers). It is known that $Mn(OH)_2$ can oxidize in air what indicated by its solution darkening. Thus, the $Mn(OH)_2$ formation colloids should be assumed also. To examine such possibility control solutions of MnS and $Mn(OH)_2$ were prepared without L-cys at the same $[Mn^{2+}]$ as in the solutions NN1-6. Such synthesized red-brown $Mn(OH)_2$ precipitate differs clearly from the pink MnS one that had occurred immediately after the components mixing.

The UV-vis absorbance spectra of the as-prepared uncapped $Mn(OH)_2$ and MnS control solutions are shown in Fig. 1c. The spectrum of the pure $Mn(OH)_2$ polydispersed solution is characterized by some peacks (λ_{max} ranged 200÷260 nm) in wider spectral range in comparison with the "pure" MnS colloid. The broad absorption band of the $Mn(OH)_2$ solution obviously means a wide distribution of the particles sizes. It should be noted that such coincidence of the MnS and $Mn(OH)_2$ control solutions absorbance spectra partly complicated the optical data interpretation.

Additional experiments show that emerald colour that occurs during the synthesis of MnS/L-cys solutions is associated with Mn/L-cys complex formation in basic media. Really, after adjustment of the L-cys solution (taking *c. n.*= 2) up to pH ≥ 9 by 0.1 M NaOH following by addition of a proper volume of Mn^{2+}-ions solution the obtained mixture became the same emerald as in the 3-components solution preparation case. Fig. 1d demonstrates an appearance of the peak at 320 nm in the emerald solution of the Mn/L-cys complexes in the basic media only which is absent in the spectra of the 3-components mixtures (Fig.1, a and b).

The recorded AFM micrographs of the deposited in the control experiments MnS and $Mn(OH)_2$ sediments at different projections and magnification are shown in Fig. 2, a and b. All the figures have close to parallelepiped morphology and demonstrate a tendency to aggregation. More clearly such tendency one can see in the 2D AFM image of quasi-spherical in shape MnS/L-cys NPs

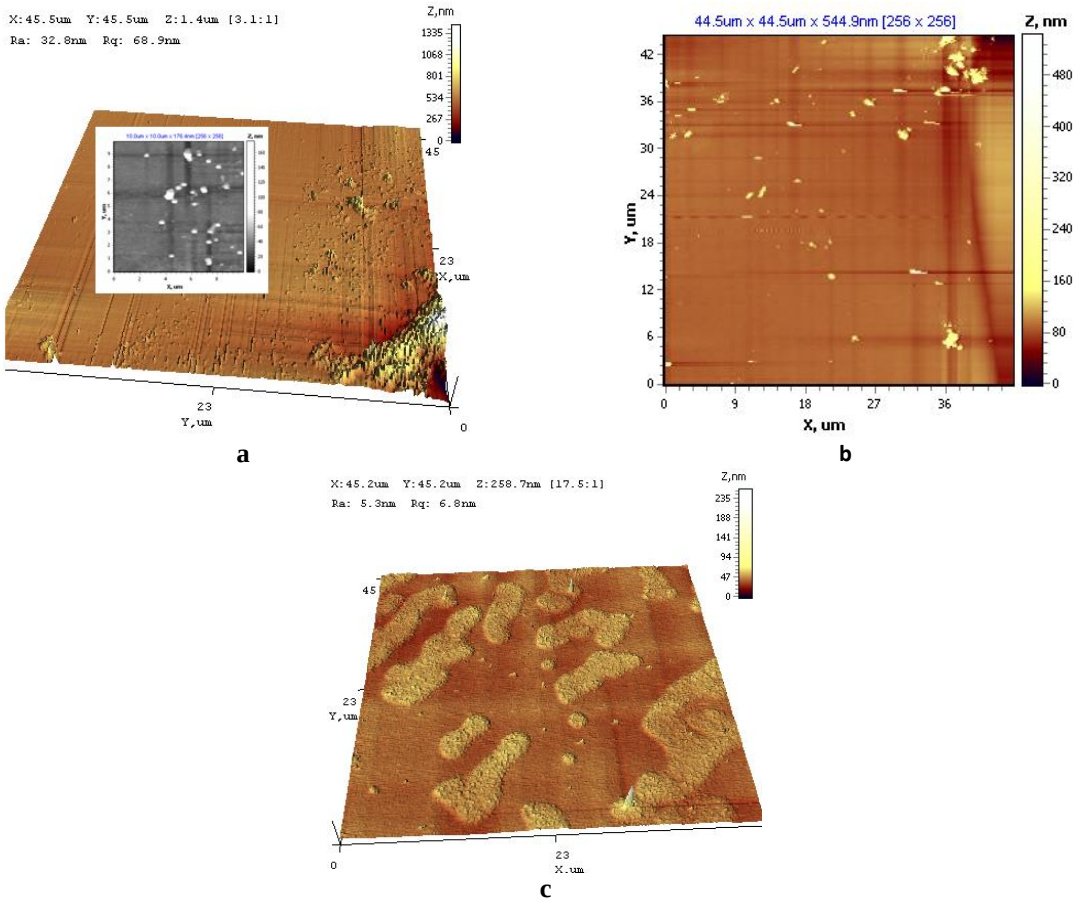

Fig. 2. a – three-dimensional (and two-dimensional in the insert) AFM-image of the MnS sediment without any capping substance; b – two-dimensional AFM-image of the $Mn(OH)_2$ deposited in the control solution; c – the MnS/L-cys NPs ($[Mn^{2+}]$: [L-cys]:$[S^{2-}]$ = 1:2:1).

(Fig. 2c) with sizes about 5-20 nm.

2.1.2. Series B.

Since the MnS/L-cys NPs yield in previous series was small the precursor concentration was increased in order to ensure the double excess of S^{2-} in Series B. This change intensified markedly the $[Mn(L\text{-}cys)_n]^{2+}$ and S^{2-} interaction and shows some different results. Though similarly to observe in previous Series A the emerald color at first observed at the solutions mixing, however it followed not only by rapid change to pink but precipitation of pink loose sediment soon. Obviously, the precipitation means that the cation and anion concenration product (CP) substantially exceeded the solubility product ($CP([Mn^{2+}][S^{2-}]) = 3{,}125\cdot10^{-4}M^2$, and K_{SP} (MnS) $= 3\cdot10^{-10}M^2$) in this case and L-cys stabilizing effect had diminished.

Precipitate rinsed several times with deionized water and dried. According to the EDX data the precipitate consists on everage on 31.1 mas. % of Manganese, 20.3 mas. % of Sulfur and 48.6 mas. % of Oxygen, that confirmed the MnS formation at this experiment. Meanwhile high Oxygen percent reflects presense of $Mn(OH)_2$ or/and various Manganese oxydes such as Mn_2O_3 and Mn_3O_4 in the product.

2.2. MnS/TGA NPs synthesis

Thioglycolic acid easily oxidizes to the dithiodiglycolic acid in presence of Mn^{2+}-ions in basic aqua media:

$$2\,HSCH_2CO_2H + O \rightarrow [SCH_2CO_2H]_2 + H_2O \qquad (4)$$

However it was asserted in [21] about formation in basic media of two presumably chelates mono- and bis-thioglycolate complexes ($MnSCH_2CO_2$, Log $K_{f,1}$=4.4 and $[Mn(SCH_2CO_2)_2]^{2-}$, Log $K_{f,2}$ = 7.6). At that time, it was noted in [21] that optical properties of their aqueous solutions didn't confirmed this conclusion because the beginning of a band in an absorbance spectrum was observed in the same region in which the free divalent thioglycolate ion absorbs. Thus, the $[Mn(SCH_2CO_2)_2]^{2-}$ complexes formation retained questionable.

To compare effect of pH on MnS NPs formation with TGA as capping agent our studies were done at first at the $[Mn^{2+}]$:$[S^{2-}]$ = 1:1 ratio, *c. n.* = 2 in basic, neutral and acidic media. Complex formation between Mn^{2+}-ions and TGA was studied at pH = 7; 9; 10 and 11 adjusting proper pH by 0.1M NaOH solution. Primary transparent the Mn/TGA stock solutions (pH = 7) became carmine pink after adjusting pH up to 9÷11 however soon all solutions became colourless (except light yellow-pink color at pH=11). Difference between the absorbance spectra of the Mn^{2+}-ions, free TGA and Mn/TGA solutions gives base to conclude about the complexes formation at pH = 9, 10 and 11.

Introduction to the flasks with the Mn/TGA solutions the proper volume of the Na_2S solution immidiately causes pink shade appearance at pH=11 only. However after a day a fluffy pink sediment observed in the flask bottom at

pH= 9 and 10 also.

The obtained MnS/TGA NPs absorbance spectra (Fig. 3, a) are characterised by the overlap between two spectra with maxima at 210±5 and 235±5 nm when $[Mn^{2+}]:[S^{2-}]$ = 1:1, *c. n.* = 2 and pH of stock Mn/TGA solutions was equal 7÷11. The long absorption tails in long-wave region that observed with time are probably due to the NPs wide size scattering. As one can see the absorbance spectra in Fig. 3a practically coinsided that demonstrated the independence of the results on the colloids' pH ranged 7 ÷11.

2.2.1. Series A.

Set experiments were carried out without use of additional NaOH solution taking into account that the Na_2S stock solution is basic (pH = 11). Effect of the precursors content on the absorbance spectra positions is shown at Fig. 3b. Comparison of Figs. 3a and 3b demonstrates reproducing of the peaks at 210±5 and 235±5 nm. Similar maximum at 205 nm on the spectra of the control MnS solution (Fig. 3a) firmed the conclusion about the MnS/TGA NPs presence it all cases. However, the "left" side of the spectrum is less responsive to changes in the composition of the mixture than the "right" side. Increase of the absorbance at λ_{max} ~ 250 nm intencity with TGA content (in direct of *c.n.* from 2 to 6) can be connected with doubly deprotonated species storage in the basic solutions. Really pure TGA is doubly deprotonated at pH = 11.5 (pKa_{COOH} = 3.67; pKa_{SH} = 10.31) that according to [22] show peaks in the UV–vis absorbance spectra at 185 and 250 nm. The maximum near λ_{max} ~ 250 nm can show presence of free doubly deprotonated species (−S-CH_2-COO−) in the 3-component solutions.

As it is seen in Fig. 3b the spectra band position varies also with the crystal-forming components concentration. The UV-vis spectra of the colloids with $[Mn^{2+}]:[TGA]:[S^{2-}]$ = 1:2:1 and 1:4:1 almost coincided demonstrating the smallest NPs formation. The largest NPs are synthesized at 1:2:2 ratio. Doubling of $[S^{2-}]$ increases the absorbance and the band positions shifted to longer waves obviously due to larger sizes of the Mn-containing NPs.

2.2.2. Series B.

Interaction of the Na_2S with Mn/TGA had resulted immediately in pink color of the mixture followed by pink-peach like hue and precipitates. Later (after four hours) a green-grey sediment formed at the flask bottom. Probably, the MnS nanocrystals transformation into other modification had occurred.

Meanwhile, EDX obtained that the green-grey precipitate in the solution with 1:2:2 ratio consists of 36.6 mass % Mn; 17.2 mass % S and 46.2 mass % O. Here S and Mn elements can be assigned to MnS formation. High percent of Oxygen witnesses presence of other Oxygen-containing compounds of manganese.

2.3. MnS/citrate NPs synthesis

2.3.1. Series A.

According to [23] many different mono- and polynuclear coordination modes are revealed for manganese (II) citrate complexes. In this work, room temperature synthesis of the MnS/citrate NPs was done at the same coordination number for the ligands as in previous colloids and ratio of the crystal-forming precursors (see Table 1). Since anhydrous trisodium

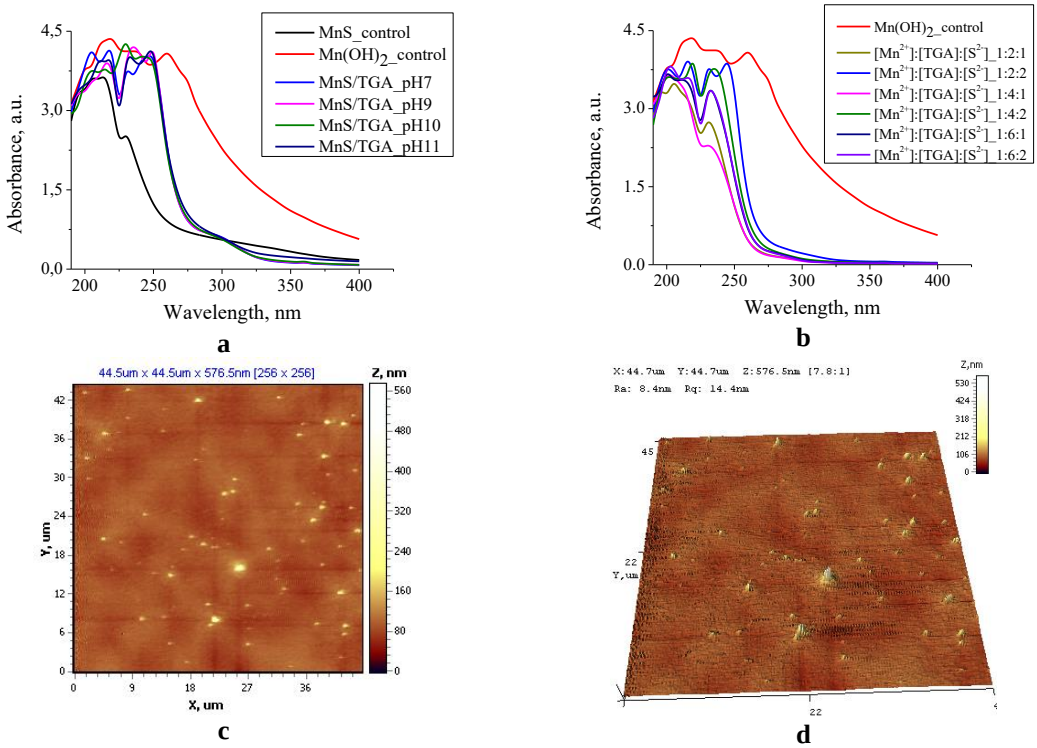

Fig. 3. a – the UV–vis spectra of the MnS/TGA (1:2:1 ratio, *c.n.*=2) colloids at pH= 7÷ 11 (see legend) in comparison with the MnS and $Mn(OH)_2$ control solutions spectra; b – the absorbance spectra of the MnS/TGA (Series A) colloids and $Mn(OH)_2$ control solution; c, d – two- and three-dimensional AFM image of the MnS/TGA (1:2:1) NPs Series A).

citrate and Na_2S stock solutions are basic – the proper volume of all colour-free precursors solutions were mixed firstly without their pH adjustment. The obtained transparent colour-free mixtures became pink and turbid on second day for molar ratio $[Mn^{2+}]:[S^{2-}]$ = 1:2 at *c. n.* = 2, 4, and 6, respectively, and stayed without changes for molar ratio $[Mn^{2+}]:[S^{2-}]$ = 1:1.

Low nanocrystals growth and focusing of size distribution were observed soon after the precursors mixing, while further storage of the solutions resulted in ripening process and broadening of the size distribution at $[Mn^{2+}]:[S^{2-}]$ = 1:1, *c. n.*= 2 and 4. (Fig. 4a). The "magic" ratio $[Mn^{2+}]:[S^{2-}]$ = 1:2 manifested itself also in the citrate-ions presence case by accelerating of pink products formation at all *c.n.* and λ_{edge} shift to longer waves. Note that sharp the MnS NPs spectrum edge steepness confirms the capping action of citrate-ions.

The UV-vis absorbance spectra of the 3-components solutions are bimodal with $\lambda_{max.}$ = 215 and 230 nm at stoichiometric Mn and S ratio and 245 nm and 235 nm in double sulphur-ions excess presence (Fig. 4a). Complicated view of the UV–vis absorbance spectra similar to presented in Fig. 4a was treated in [11] as formation of β- and γ-MnS/citrate NPs where two absorbance peaks about 206÷232 nm and 263÷265 nm as well as the broad absorption extending up to 800 nm were observed. However we take into account that the peaks positions are close to $\lambda_{max.}$ = 220 and 240 nm in the $Mn(OH)_2$ control solution spectra which almost coincided with the MnS/citrate spectra in Fig. 4a.

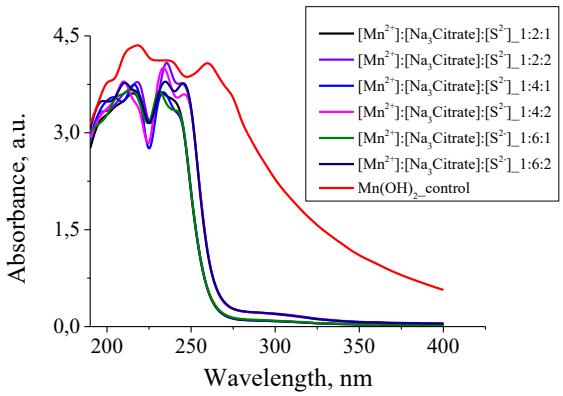

a

Fig. 4. a – the absorbance spectra of the MnS/citrate solutions (Series A) (see legend) in comparison with the uncapped $Mn(OH)_2$ control solution spectra.

2.3.2. Series B.

The precursors' mixing is followed by fast peach color sediments occurrence. The chemical composition of as-prepared samples with $[Mn^{2+}]:[citrate]:[S^{2-}]$=1:2:2 was determined by EDS that revealed 18.0 mass% S, 34.9 mass % Mn and 47.1 mass % O. Presence of Sulfur in the specimen can be an important argument according to the MnS NPs formation because the capping agent is sulfur-free contrary to the thiols L-cys and TGA. At the same time, the formation of manganese hydroxide and/or oxides cannot be ruled out.

Conclusions

The aim of the study was to investigate the interactions in the 3-component system (Mn^{2+} -stabilizer-S^{2-}), as well as to analyze their effect on optical properties, growth and size of formed MnS NPs and compare the stabilizing effect of capping agents: L-cys, TGA and citrate aqueous solutions.

All three capping agents belong to the same class of organic compounds, namely carboxylic acids, and L-cys and TGA contain SH-functional groups, and L-cys also has NH_2-group, while, the citrate-ion has only carboxyl groups. All experiments were performed under the same conditions (temperature, preparation of primary solutions, the order of mixing, and the ratio of components $[Mn^{2+}]:[S^{2-}]$ = 1:1 and $[Mn^{2+}]:[S^{2-}]$ = 1:2 with *c. n.* 2, 4, and 6) for all potential complex agents.

Analysis of the optical properties suggests that all three substances are suitable for use as capping agents in the synthesis of MnS NPs. It was found that the increase in *c. n.* from 2 to 6 does not change the pattern of absorption spectra at the ratio $[Mn^{2+}]:[S^{2-}]$ = 1:1, but there is a noticeable shift to the long-wavelength range at the ratio $[Mn^{2+}]:[S^{2-}]$ = 1:2, which is in a good agreement with the literature data [1], which confirms the dominant effect of anion concentration on the rate of nucleation and growth of MnS NPs.

In addition, the effect of the concentration of the primary precursors is significant. When it is increased by an order of magnitude, the stabilizing effect of the used capping agents is destroyed and pink precipitate MnS observed, which over time turns brown, probably oxidizing to $Mn(OH)_2$ and various manganese oxides. The presence of manganese, sulfur and oxygen in the investigated powders was proved by EDX analysis of the samples, which confirms the previous hypothesis.

From the analysis of the absorption spectra of MnS NPs obtained at different pH, we assume that pH effect on the formation of the final products is negligible, at that time at the stage of the $[Mn(Ligand)_n]^{n+}$ complex formation at pH ≥ 9 in the presence of SH-containing capping agents new peaks at 320 nm (for L-cys) and 335 nm (for TGA) are emerged, which confirms the formation of the corresponding complexes. No such peaks are observed when the citrate-ions are used regardless of pH value. Analysis of the spectra shows that the sizes of the MnS NPs stabilized by L-cys and TGA are almost equal (3-5 nm), and those of citrate ion stabilized are smaller (2-3 nm).

Formation of $Mn(OH)_2$ in aqua media occurs together with MnS, because K_{sp} of MnS and $Mn(OH)_2$ are very similar.

Pylypko V.G. **–** PhD student at the Department of General Chemistry and Chemical Materials Science;
Krupko O.V. **–** Candidate of Chemical Sciences, Assistant Professor of the Department of Medical and Pharmaceutical Chemistry;
Fochuk P.M. – Doctor of Chemical Sciences, Professor of the Department of General Chemistry and Chemical Materials Science.

[1] A. M. Ferretti, S. Mondini, and A. Ponti, *Manganese Sulfide (MnS) Nanocrystals: Synthesis, Properties, and Applications*, Advances in Colloid Science (2016); https://doi.org/10.5772/65092.
[2] Dan Xu, Ranran Jiao, Yuanwei Sun, Dezhi Sun, Xianxi Zhang, Suyuan Zeng, *L-Cysteine-Assisted Synthesis of Urchin-Like γ-MnS and Its Lithium Storage Properties*, Nanoscale Research Letters, 11, 444 (2016); https://doi.org/10.1186/s11671-016-1664-6.
[3] T. He, , X. Qin, C. Jiang, D. Jiang, S. Lei, J. Lin, … P. Huang, *Tumor pH-responsive metastable-phase manganese sulfide nanotheranostics for traceable hydrogen sulfide gas therapy primed chemodynamic therapy*, Theranostics, 10(6), 2453 (2020); https://doi.org/10.7150/thno.42981.
[4] Jianping Ge and Yadong Li, *Controllable CVD route to CoS and MnS single-crystal nanowires*, Chem. Comm., 19, 2498 (2003); https://doi.org/10.1039/B307452H.
[5] J. Mu, Z. Gu, L. Wang, Z. Zhang, H. Sun, & S.-Z. Kang, *Phase and shape controlling of MnS nanocrystals in the solvothermal process*, J. Nanopart. Res., 10, 197 (2007); https://doi.org/10.1007/s11051-007-9216-8.
[6] P. Zhao, Q. Zeng, X. He, H. Tang, & K. Huang, *Preparation of γ-MnS hollow spheres consisting of cones by a hydrothermal method*, J. Cryst. Growth, 310(18), 4268 (2008); https://doi.org/10.1016/j.jcrysgro.2008.06.076.
[7] J. Lu, P. Qi, Y. Peng, Z. Meng, Z. Yang, W. Yu, & Y. Qian, *Metastable MnS Crystallites through Solvothermal Synthesis*, Chem. Mat., 13(6), 2169 (2001); https://doi.org/10.1021/cm010049j.
[8] K. Qi, R. Selvaraj, U. Jeong, Salma M. Z. Al-Kindy, M. Sillanpää, Y. Kim, & C. Tai, *Hierarchical-like multipod γ-MnS microcrystals: solvothermal synthesis, characterization and growth mechanism*, RSC Advances, 5, 9618 (2015); https://doi.org/10.1039/c4ra16038j.
[9] S. H. Chaki, M. P. Deshpande, J. P. Tailor, K. S. Mahato, & M. D. Chaudhary, *Wet Chemical Synthesis and Characterization of MnS Nanoparticles*, Adv. Mater. Res., 584, 243 (2012); https://doi.org/10.4028/www.scientific.net/amr.584.243.
[10] K. Qi, Y.-Q. Wang, S. Rengaraj, B. Al Wahaibi, & A. R. M. Jahangir, *MnS spheres: Shape-controlled synthesis and its magnetic properties*, Mater. Chem. Phys., 193, 177 (2017); https://doi.org/10.1016/j.matchemphys.2017.02.023.
[11] T. Veeramanikandasamy, K. Rajendran, & K. Sambath, *Influence of Mn/S molar ratio on the microstructure and optical properties of MnS nanocrystals synthesized by wet chemical technique*, J. Mater. Sci.: Mater. Electron., 25(8), 3383 (2014); https://doi.org/10.1007/s10854-014-2029-5.
[12] M.Pnjr, K.V.Anandb, Dr. V.J.K.Kishor Sonti, V.Kannana, Chennai, *A facile room temperature synthesis of MnS nanostructured materials using starch as capping agent with improved optical properties*, Conference: International Conference on Advanced Materials and its Applications (ICAMA-2011), 2011.
[13] J. Zhang, R.Shi, C. Zhang, L. Li, J. Mei, & S. Liu, *Solvothermal synthesis of manganese sulfides and control of their phase and morphology*, J. Mater. Res., 1 (2018); https://doi.org/10.1557/jmr.2018.365.
[14] S. Shabna, Intern. J. Sci. Res., *Confirmation and Characterization of MnS Nanocomposites*, Synthesis, 6(12), 910 (2017); https://doi.org/10.21275/ART20178701.
[15] M. Edrissi and M. Soleymani, *Stearoyl Piperidinium Chloride and Palmitoyl Piperidinium Chloride Surfactants: Synthesis, Characterization and Application as Capping Agent in the Mikroemulsion Synthesis of MnS*, Tenside Surfactants Detergents, 49(4), 335 (2012); https://doi.org/10.3139/113.110200.
[16] F. M. Michel, M. A. A. Schoonen, X. V. Zhang, S. T. Martin, and J. B. Parise, *Hydrothermal Synthesis of Pure α-Phase Manganese (II) Sulfide without the Use of Organic Reagents*, Chem. Mater., 18(7), 1726 (2006); https://doi.org/10.1021/cm048320v.
[17] N. B. Brahima, N.B.H. Mohameda, M. Poggi, R.B. Chaâbanea, M. Haouari, H.B.Ouada, M. Negreriec, *Interaction of l-cysteine functionalized CdSe quantum dots with metallic cations and selective binding of cobalt in water probed by fluorescence*, Sensors and Actuators B: Chemical, 243, 489 (2017); https://doi.org/10.1016/j.snb.2016.12.003.
[18] G. Berthon, *The stability constant of metal complexes of amino acids with polar side chains*, Pure and Appl. Chem., 67(7), 1117 (1995); http://dx.doi.org/10.1351/pac199567071117.
[19] Ebrahim Ghiamati, Faezeh Sheikhani and Alireza Farrokhi, *Potentiometric and Thermodynamic Studies of Some Metal–Cysteine Complexes*, J. Chinese Chem. Soc., 65(2), 1 (2017); https://doi.org/10.1002/jccs.201700022.
[20] Handbook of chemistry and physics, ed. D.R. Lide. 87th edition, Taylor & Francis. 2006-2007, P. 8-121.
[21] D. L. Leussing, *The Stabilities and Absorption Spectra of Complexes of Some Divalent Metal Ions of the First Transition Series with the Thioglycolate Ion*, J. Amer. Chem. Soc., 80(16), 4180 (1958); https://doi.org/10.1021/ja01549a016.
[22] A. R. Attar, D. E. Blumling, & K. L. Knappenberger, *Photodissociation of thioglycolic acid studied by femtosecond time-resolved transient absorption spectroscopy*, J. Chem. Phys., 134(2), 024514-1 (2011); https://doi.org/10.1063/1.3526746.
[23] Yuan-Fu Deng & Zhao-Hui Zhou, *Manganese citrate complexes: syntheses, crystal structures and thermal properties*, J. Coordin. Chem., 62(5), 778 (2009); https://doi.org/ 10.1080/00958970802376257.
[24] O. V. Krupko, A. G. Voloshchuk, L. P. Shcherbak, *Thermodynamic analysis of state diagrams of the MnS-H2O system*, Physics and chemistry of solid state, 10(4), 867 (2009).

В.Г. Пилипко[1], О.В. Крупко[2], П.М. Фочук[1]

Вплив стабілізаторів на оптичні властивості і стабільність наночастинок MnS

[1]*Чернівецький національний університет імені Юрія Федьковича, вул. Коцюбинського, 2, Чернівці 58012, v.pylypko@chnu.edu.ua*
[2]*Буковинський державний медичний університет, Чернівці, Україна, 58002; krupkoo@ukr.net*

Дві тіоловмісні кислоти (L-цистеїн і тіогліколева), а також цитрат-аніон були використані в якості координуючих реагентів для контролю зародкоутворення і росту наночастинок MnS при різних значеннях pH у водному середовищі. Характеристику властивостей отриманих колоїдних розчинів проводили за допомогою УФ-видимої спектроскопії та атомно-силової мікроскопії. Масову частку елементів оцінювали за допомогою енергодисперсійного рентгенівського випромінювання. Досліджено вплив молярного співвідношення кристалформуючих іонів (Mn^{2+} і S^{2-}), а також природу та вміст (координаційне число лігандів *с. п.* = 2; 4 і 6) обраних стабілізаторів на спектри поглинання. Отримано, що кількість іонів Mn^{2+} та к.ч. стабілізаторів, необхідних для ефективного покриття наночастинок MnS, близькі у трьох досліджуваних випадках. Обговорено високу ймовірність утворення $Mn(OH)_2$ як додаткового продукту взаємодії сульфіду натрію з хлоридом мангану у водному середовищі.

Ключові слова: наночастинки манган (II) сульфіду, синтез, L-Цистеїн, тіогліколева кислота, цитрат-іони, спектри поглинання, атомно-силова мікроскопія, енергодисперсійний рентгенівський аналіз.